

## 8.0 ANALYSIS OF UPPER RESERVOIR BARRIERS

Each of the physical Barriers cited on *Table 6-1* have been analyzed from the perspective of the postulated failure modes indicated thereon. As it was not practical to measure each of the parameters necessary for precise analysis, we performed a series of parametric analyses over the range of parameters deemed appropriate based on judgment, values cited in the professional literature and actual observations and measurements obtained from the field.

Following the discussion of the analyses completed, we summarize each of the physical Barriers and cite the impact of each in terms of Root Cause or Contributing Cause. As defined herein, a root cause is a cause that directly caused the Event and a primary, secondary or tertiary contributing cause is a cause that may have contributed to, but would not, either singularly or in combination with other primary, secondary or tertiary causes, have caused the Event. The descriptor primary, secondary or tertiary reflects our assessment of the degree that the cause contributed to the Event, with a tertiary cause having little or no effect on the Event

### 8.1 OVERTOPPING ANALYSIS

The initial task in our overall analysis effort was to develop an understanding of the portions of the Dike where overtopping occurred on December 14, 2005 and the magnitude of flow at these overtopping zones. This task was undertaken with a study of the most recent elevation survey of the top of the Parapet Wall as provided by AmerenUE. For Wall Segments 70 through 100 where AmerenUE has no recent survey data exists, the elevation of the top of each wall segment was estimated using the average Parapet Wall height, the maximum settlement between 2003 and 2005, and the elevation of monuments on the crest of the Dike in 2003. Using these elevations, flow was estimated by approximating each wall segment as a broad-crested weir. The highest level of water in the Upper Reservoir on December 14, 2005 was estimated at 1597.63 based on the Siemens report provided in *Appendix A*. At this elevation, overtopping of the parapet wall will occur at the locations shown on *Figure 8-1* with the corresponding flows for each area. Details of flow characteristics at the lowest wall segment in each overtopping area are shown on *Figures 8-2* through *8-4*. Overtopping flow is a function of time at each of the four overtopping zones. Flow also continues to go into storage, thereby continuing to raise the level in the Upper Reservoir until inflow equals outflow. The time at which the upper reservoir is at 1597.00 is taken as  $t = 0$ . Results shown on *Figures 8-1* through *8-4* are for a water level of 1597.63, which occurs after approximately 10 minutes, 20 seconds at a pump rate of 2600 cfs.

Estimated Overflow at Time = 10 min 20 sec

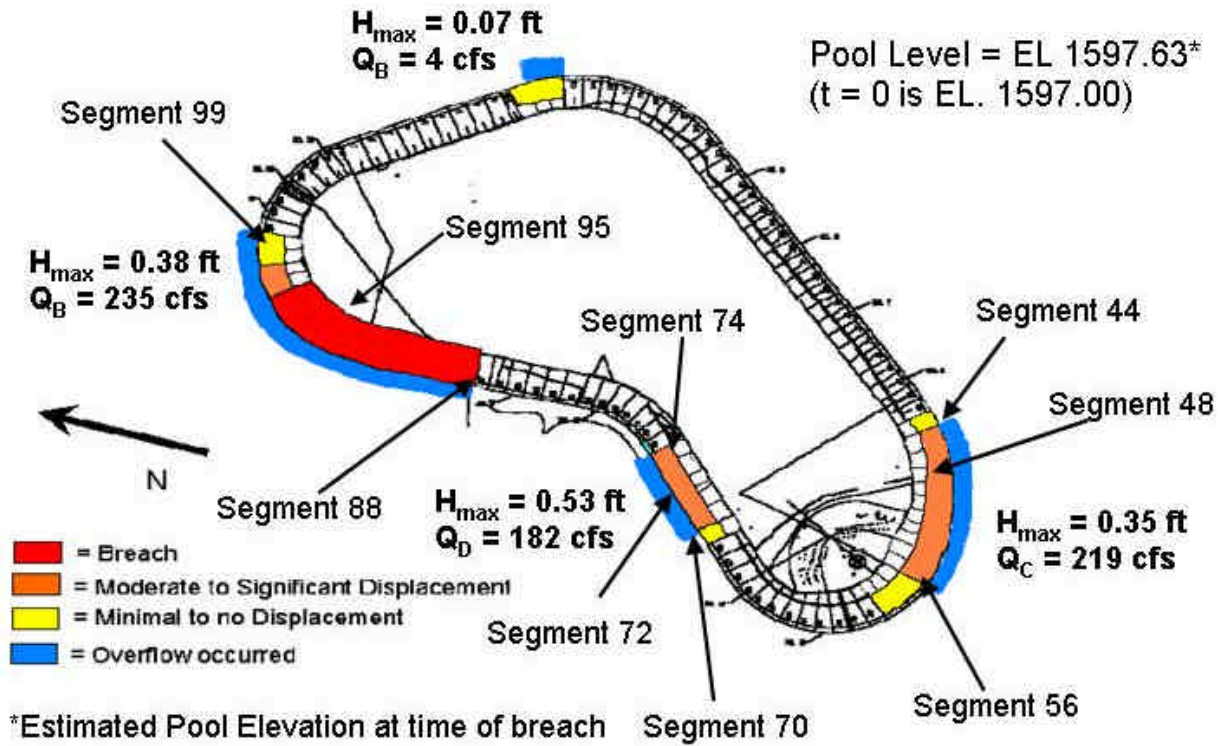
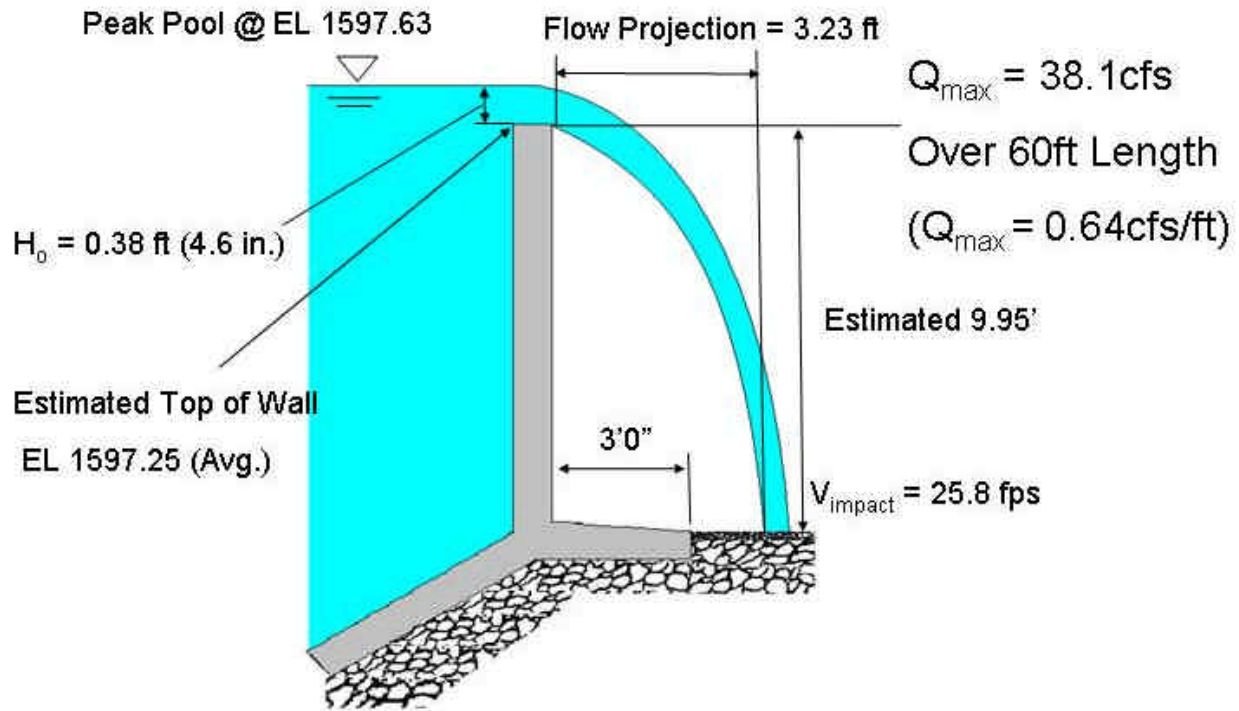


FIGURE 8-1  
OVERTOPPING ZONES

## Wall Segment 95 at Time = 10 min 20 sec



**FIGURE 8-2**

### WEIR FLOW PROJECTION – WALL SEGMENT 95

The results of the overtopping analysis shown on *Figures 8-1 and Figure 8-2* indicate that the total flow near Parapet Wall Segment 95, where the Breach occurred, is estimated to be 235 cfs at  $t \sim 10$  minutes, 20 seconds. The total flow over Wall Segment 95 (60 feet long) having an average top Elevation of 1597.25 is 38.1 cfs, or 0.64 cfs/ft. The overtopping flow rapidly infiltrated into the Rockfill Dike, resulting in a rapid rise in the phreatic surface and the pore pressure on the critical Dike/foundation interface.

The total flow over Wall Segment 72 (78 feet long) having an average top Elevation of 1597.10 is 80.1 cfs, or 1.03 cfs/ft. This is slightly greater than at the Breach Area but over a more concentrated zone. In the southwest corner as shown on *Figure 8-4* for Parapet Wall Segment 48, the flow is estimated to be 33.1 cfs over a length of 60 feet or about 0.55 cfs per foot. These

flows caused Parapet Wall Segment Nos. 72 and 48 to be undermined as illustrated below on *Figure 8-5* and *Figure 8-6* respectively.

## Wall Segment 72 at Time = 10 min 20 sec

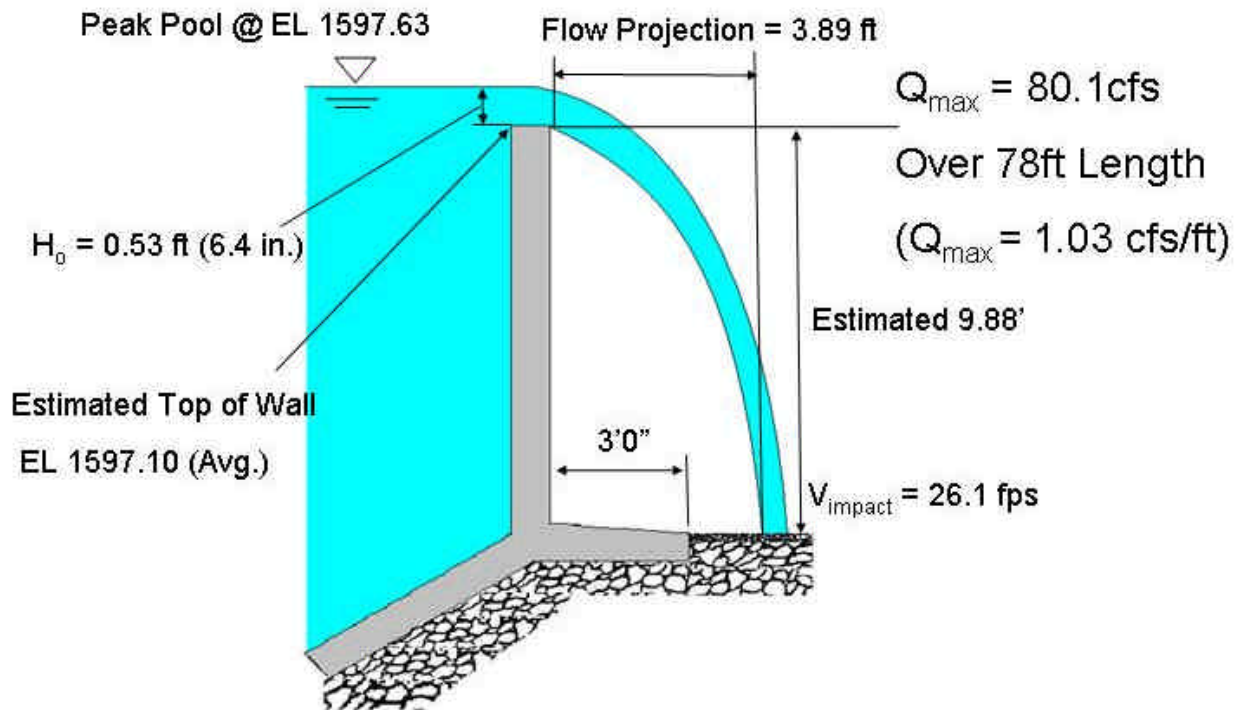


FIGURE 8-3

WEIR FLOW PROJECTION – WALL SEGMENT 72

## Wall Segment 48 at Time = 10 min 20 sec

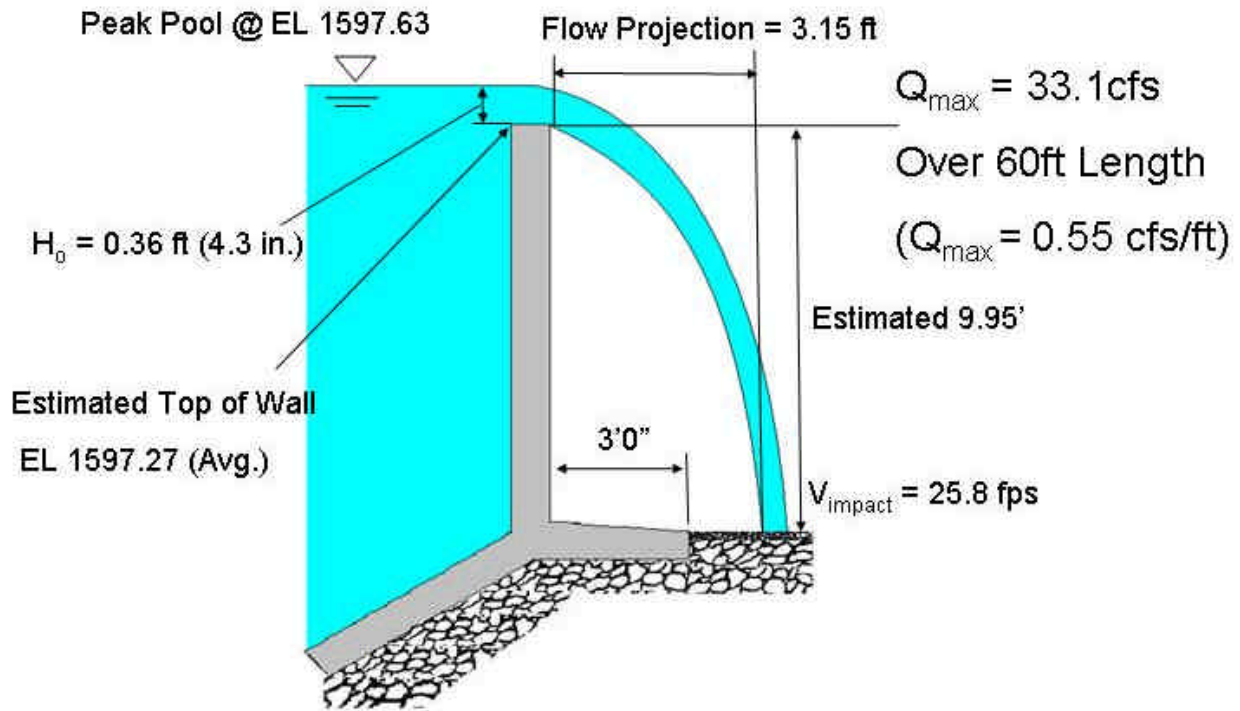


FIGURE 8-4

WEIR FLOW PROJECTION – WALL SEGMENT 48



**FIGURE 8-5**

**PARAPET WALL SEGMENT 72 UNDERMINING**



**FIGURE 8-6**

**PARAPET WALL SEGMENTS 44 TO 56 UNDERMINING**

## 8.2 PARAPET WALL STABILITY AND STRUCTURAL ANALYSIS

An analysis of the stability and structural integrity of the Parapet Wall was performed to assess the possibility that the Wall failed due to the water pressure associated with the Upper Reservoir level being in the range of El. 1598. Our analysis sets aside the question raised above as to whether it was good design practice in the 1960s to consider parapet walls on the crest of a dam in general as a means of retaining water on an “everyday” basis as opposed to storm conditions or wave conditions.

Our analysis considered six situations as follows:

- The original analysis of the Wall as presented on the construction drawing for the project.
- New overturning analysis of the Wall with the water level as high as El. 1599 with no undermining.
- New sliding analysis of the Wall with the water level as high as El. 1599 with no undermining.
- New overturning analysis of the Wall with the water level as high as El. 1599 with undermining.
- New sliding analysis of the Wall with the water level as high as El. 1599 with undermining.
- Structural analysis check of the concrete thickness and steel reinforcing.

### 8.2.1 Original Analysis of the Wall

*Figure 8-7* below is a re-print of the original analysis taken from the original construction drawings.

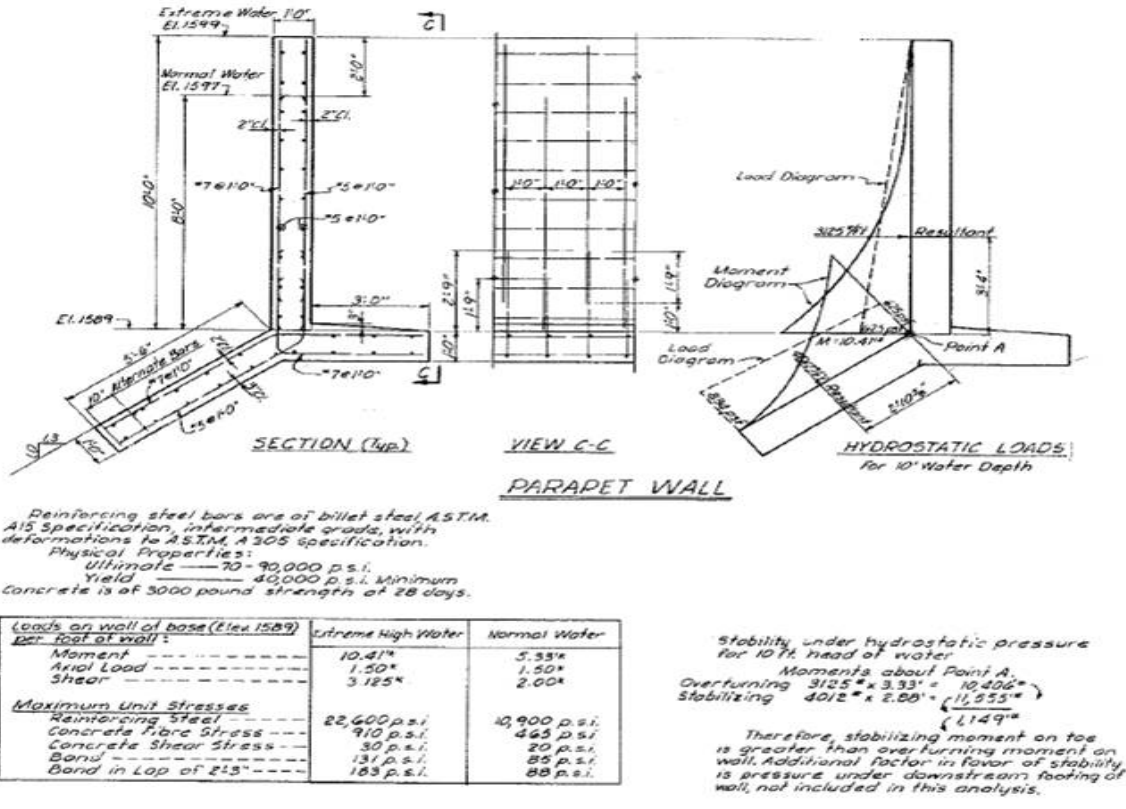


FIGURE 8-7

ORIGINAL WALL ANALYSIS

We have a few comments on this analysis. Firstly, the designer summed moments about Point A at the downstream bottom corner of the vertical stem of some of the acting forces - not all. Theoretically, one can sum moments about any point so long as all forces and moments are considered. Practitioners normally sum moments about the downstream toe, i.e., about the lower right hand corner of the base and all of the forces and moments would be considered.

Secondly, the originating analyst ignored the weight of the concrete and the soil pressure, and thirdly, the analyst ignored any uplift pressure that might develop under the foundation when the water level is in the range of El. 1598.

Our conclusion on this matter is that the original analysis would not be acceptable in a modern regulatory environment.

## 8.2.2 New Overturning Analysis with No Undermining

The forces considered for this analysis are illustrated below on **Figure 8-8** with the results shown on **Figure 8-9**. The results indicate that the Wall was stable against overturning for all practical purposes under the given water level and so long as no undermining had developed.

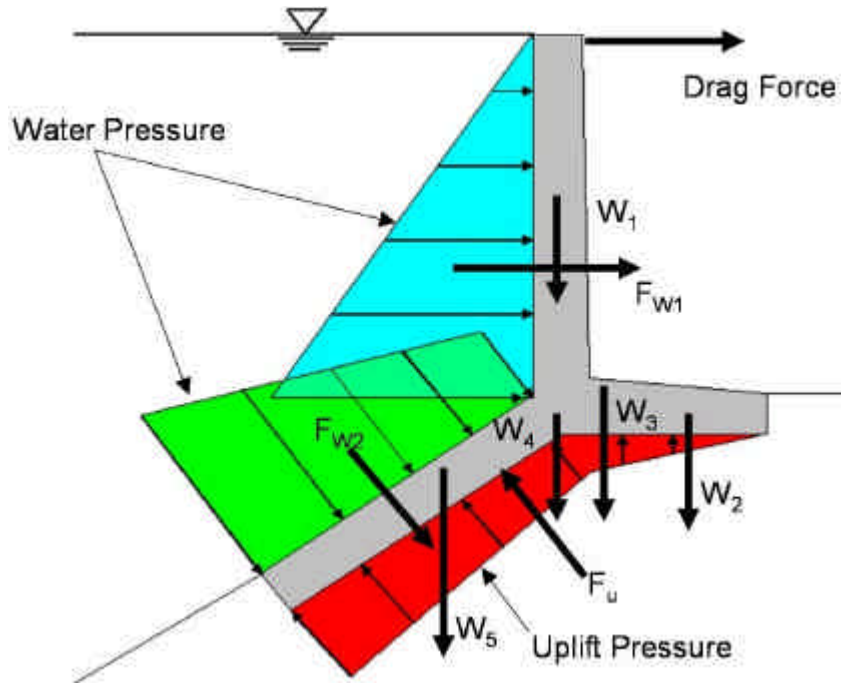


**FIGURE 8-8**

**OVERTURNING ANALYSIS WITH NO UNDERMINING**

## Factor of Safety vs. Water Elevation

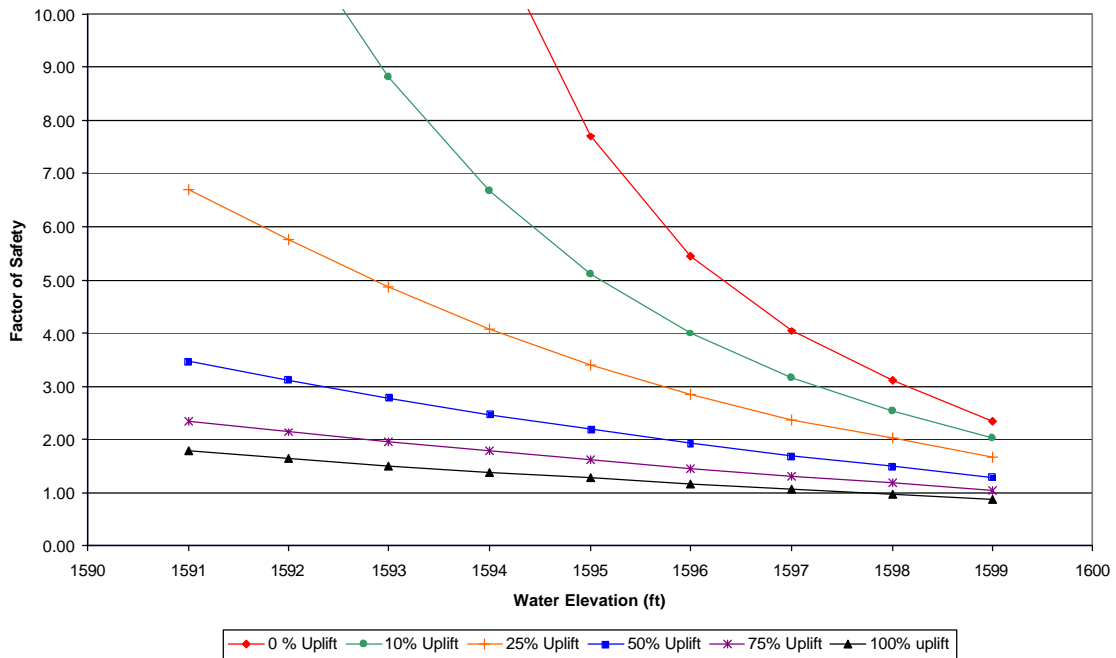


**FIGURE 8-9**

### OVERTURNING STABILITY ANALYSIS RESULTS

#### 8.2.3 New Sliding Analysis with No Undermining

The forces considered for the sliding analysis are illustrated below on *Figure 8-10* with the results shown on *Figure 8-11*. The results indicate that the Wall was stable against sliding for all practical purposes under the given water level and so long as no undermining had developed.

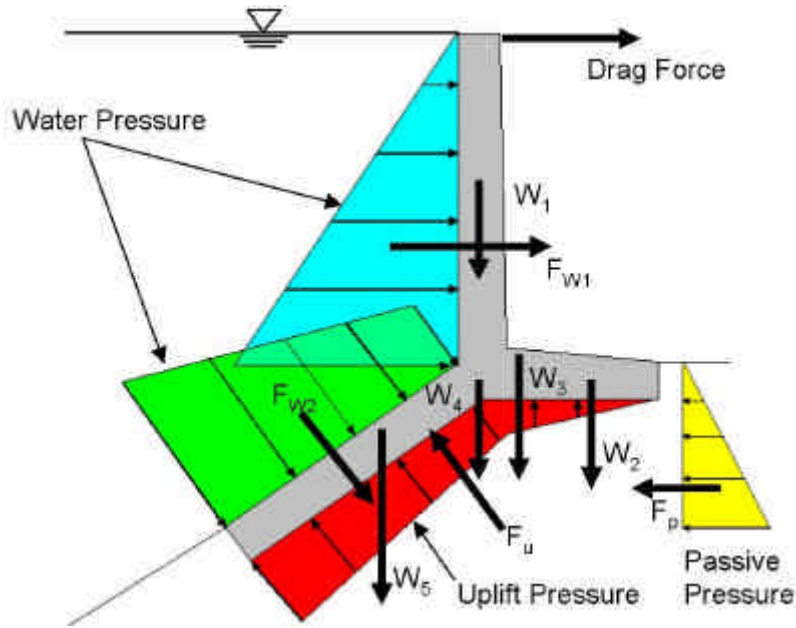


**FIGURE 8-10**

**SLIDING ANALYSIS WITH NO UNDERMINING**

***Factor of Safety vs. Water Elevation***

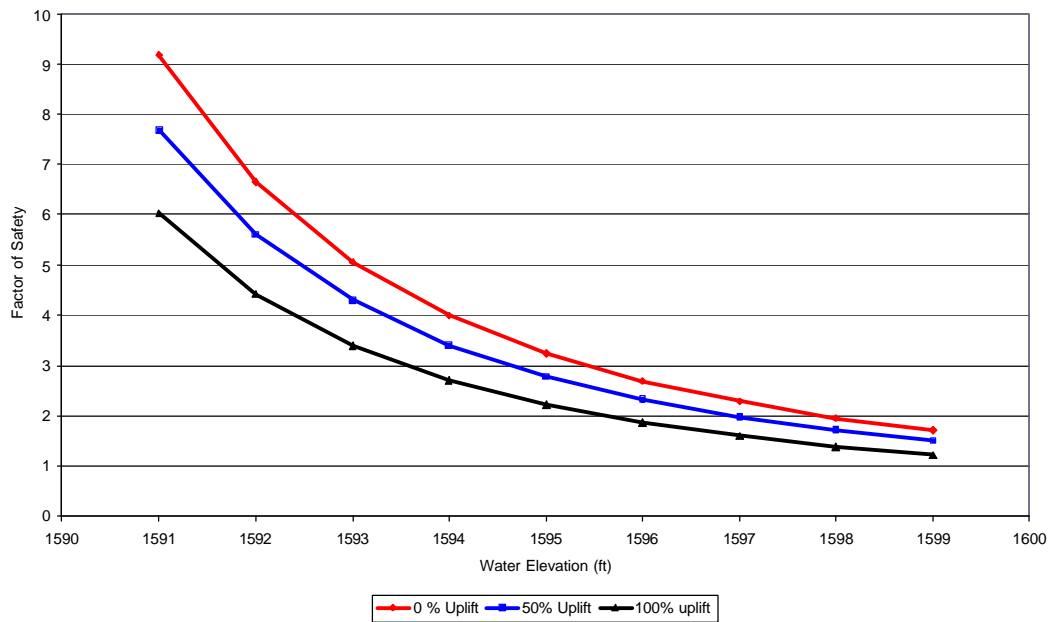


**FIGURE 8-11**

**SLIDING ANALYSIS RESULTS**

## 8.2.4 New Overturning Analysis with Undermining

The forces considered for this analysis are illustrated below on *Figure 8-12* with the results shown on *Figure 8-13*. The results indicate that the Wall becomes unstable when undercutting penetrates about three feet under the wall. This analysis is two dimensional, and therefore for the Wall segment to actually fail, the entire 60 feet long Wall Segment would have to be undermined to this degree. We observe that Wall Segment 72 shown on *Figure 8-5* was probably “saved” by three dimensional action and the Wall Segments 44 to 56 shown on *Figure 8-6* were not undermined enough to result in an unstable situation.

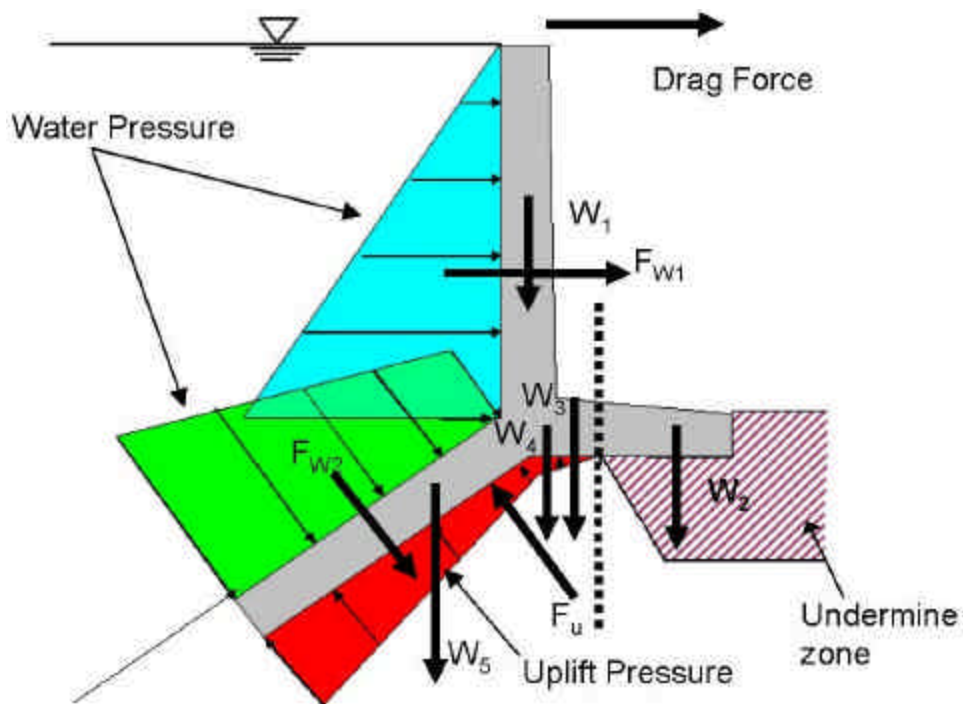


**FIGURE 8-12**

**NEW OVERTURNING ANALYSIS WITH UNDERMINING**

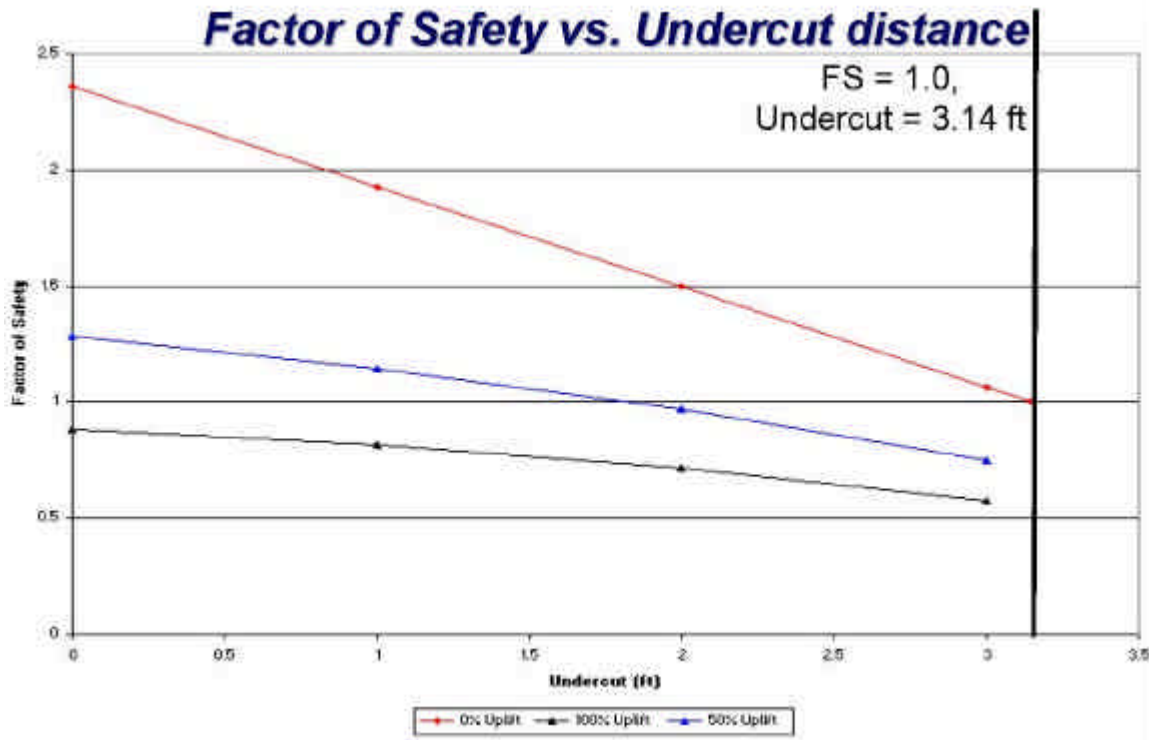


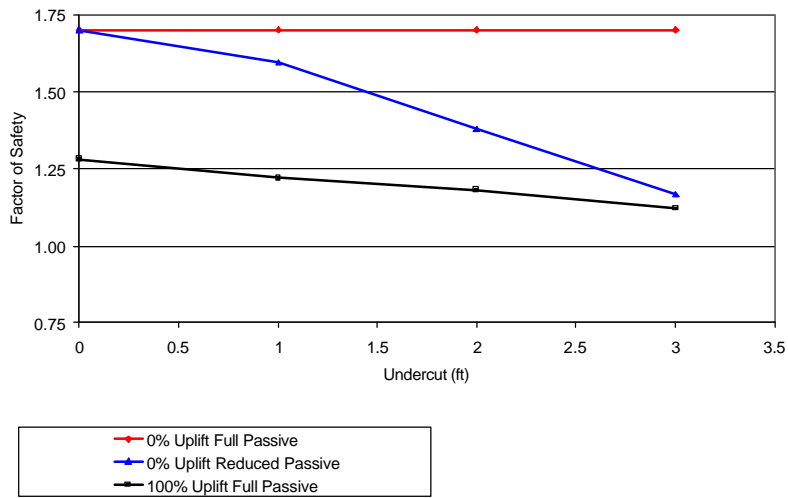
**FIGURE 8-13**

**OVERTURNING RESULTS WITH UNDERMINING**

**8.2.5 New Sliding Analysis with Undermining**

The forces considered for this analysis are illustrated are the same as shown on *Figure 8-10* for the overturning analysis and the results shown below on *Figure 8-14*. The results indicate that the Wall will probably fail first due to overturning (before sliding) when undermining occurs, primarily because of the upstream sloping base.

### **Factor of Safety vs. Undercut Distance**



\*Passive Pressure is reduced as undercut distance increases. reduction for each undercut distance is shown in the table to the right.

undercut (ft)	% of Passive Pressure
3	50
2	70
1	90
0	100

**FIGURE 8-14**

### **SLIDING RESULTS WITH UNDERMINING**

#### **8.2.6 Structural Analysis Check of Concrete and Reinforcing Steel**

Our check of the concrete stresses and reinforcing steel indicate that the Wall was adequately reinforced and that the thickness of the concrete compressing the stem and two bases is adequate.

#### **8.2.7 Summary of Analysis Results for the Parapet Wall**

Based on our analysis, we conclude the following:

- The Parapet Wall is stable for all practical purposes at water levels in the Upper Reservoir as high as El. 1599 so long as no undermining occurs.
- The Parapet Wall is marginally stable to unstable at water levels in the Upper Reservoir at El. 1599 when undercutting penetrates about three feet. Three dimensional effects, i.e., support from non-undermined



portions of a Wall Segment, tend to stabilize individual Wall Segments as is the case with Wall Segment 72.

- The Wall is adequately designed with respect concrete thickness and reinforcing steel.

In terms of the Root Cause Analysis, as defined in *Section 5.0*, the failure of the Parapet Wall may have been a secondary contributing cause to the Event. RIZZO is unable to determine if the Parapet Wall failed before the Rockfill Dike or during the failure of the Rockfill Dike. There is inadequate evidence to assess the timing of Parapet Wall Failure. If the Parapet Wall failed before the Rockfill Dike, it could have (1) led to a much more rapid rise in the phreatic surface and associated pore pressures at the Dike/foundation interface and (2) led to the surface transport of rockfill on the downstream face, thereby diminishing the effective stress at the Dike/foundation interface. If the Parapet Wall failed during the failure of the Rockfill Dike, then it was not a contributing cause.

### **8.3 SEEPAGE ANALYSIS**

The second step in our overall analysis effort was to develop an understanding of the seepage behavior and pore pressure distribution in the Rockfill Dike, especially at the critical Dike/foundation interface. This effort was undertaken with a computerized seepage analysis using the two dimensional program, SEEP2D (Boss International and Brigham Young University, 1999). We first established a “best estimate” set of properties for the Dike in the area of the Breach and the postulated a range of variability for these parameters. The range of properties was based on measurement and observation of properties in the field, judgment and values appearing in the literature.

We also used a model appropriate for the Breach Area; specifically we accounted for the increased depth to rock and the initial grout curtain, as well as the second grout curtain at this section. We also adjusted the boundary conditions of the model to account for the drainage ditch at the downstream toe of the Dike.

#### **8.3.1 Property Calibration Runs**

To check the validity and compatibility of our estimate of the basic relative permeability values, we performed a set of calibration runs. We estimated the seepage from the Upper Reservoir without the HDPE Liner (installed in 2004) and compared our results with estimated seepage

reported by AmerenUE. We then adjusted slightly our estimates to affect a reasonable match between our estimate of seepage and AmerenUE's values. The model used for this calibration model is shown on **Figure 8-15** and the phreatic surface and flow net is shown on **Figure 8-16**. Calculations are provided in **Appendix F**.

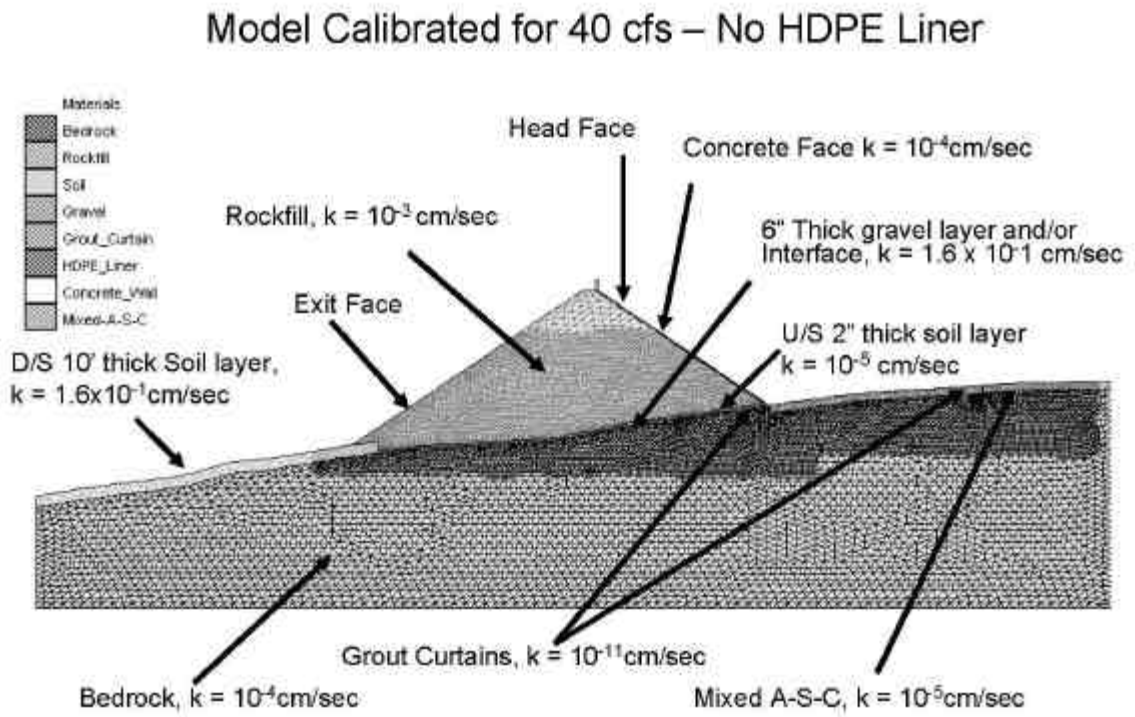


**FIGURE 8-15**

**CALIBRATION MODEL**

A comment pertaining to the calibration runs is that the overall calibration check is somewhat crude as the accuracy of the leakage rate available is limited. Specifically, the available leakage rates are such that one cannot distinguish water lost through the Dike from that lost through the bottom of the Upper Reservoir bottom or that lost through evaporation. Also, the configuration of the Dike varies significantly around the perimeter of the Upper Reservoir, whereas we considered only the geometry at the Breach Area as being reasonably indicative of all cross sections. Therefore, we are able to conclude only that our chosen parameters are in the proper range, but parametric runs as described below are necessary to fully understand the range of possible behavior of the Dike.

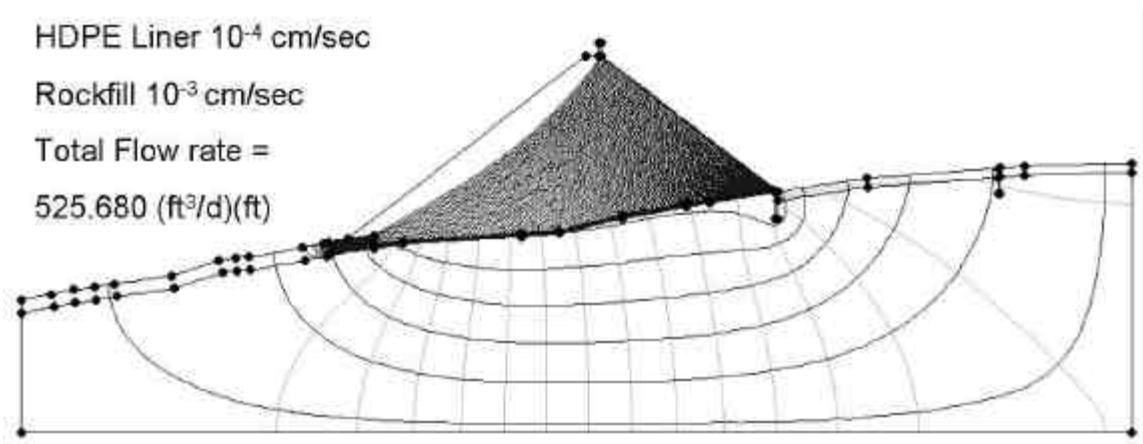


**FIGURE 8-16**

**FLOW NET FOR CALIBRATION MODEL**

A secondary observation with this model is that there are certain zones in the Dike, such as at the upstream toe, where the gradient may have been relatively high. This would suggest the possibility of fines transport within the Dike itself, i.e., movement of fines from the toe area toward the center of the Dike. Except for the small zone at the extreme downstream toe, the gradients were too low to move the fines through the Dike entirely. This observation is consistent with reports by AmerenUE that major quantities of fines were not observed in the Pump-Back Pond at the southeast corner of the Upper Reservoir, the sink for the toe drainage ditch. RIZZO personnel observed only minor quantities of fines buildup in portions of the drainage ditch, e.g., in the reach below Parapet Wall Segment 72.

Therefore, while some fines transport and subsequent clogging of the filters near to the upstream toe of the embankment would have theoretically been possible, clogging of the filters in this area would have not had a substantial impact on the phreatic surface at the downstream toe. Additionally, the gradients shown in *Figure 8-16* and field observations suggest that clogging of the filters under the downstream slope of the Dam did not occur.

**8.3.2 Best Estimate and Parametric Runs**

After calibrating the model shown on *Figure 8-15* and adding the HDPE Liner on the upstream face of the Dike, we performed a series of seepage analysis runs on the “Best Estimate” Model developed on *Figure 8-15* and modified to include the HDPE/LDPE Liner as shown in *Figure 8-17*. The resulting flow net shown on *Figure 8-18* indicates that the Liner significantly changed

the flow regime, dropping the phreatic surface to the level of the interface. This change increases the factor of safety for wedge failures along the interface significantly.

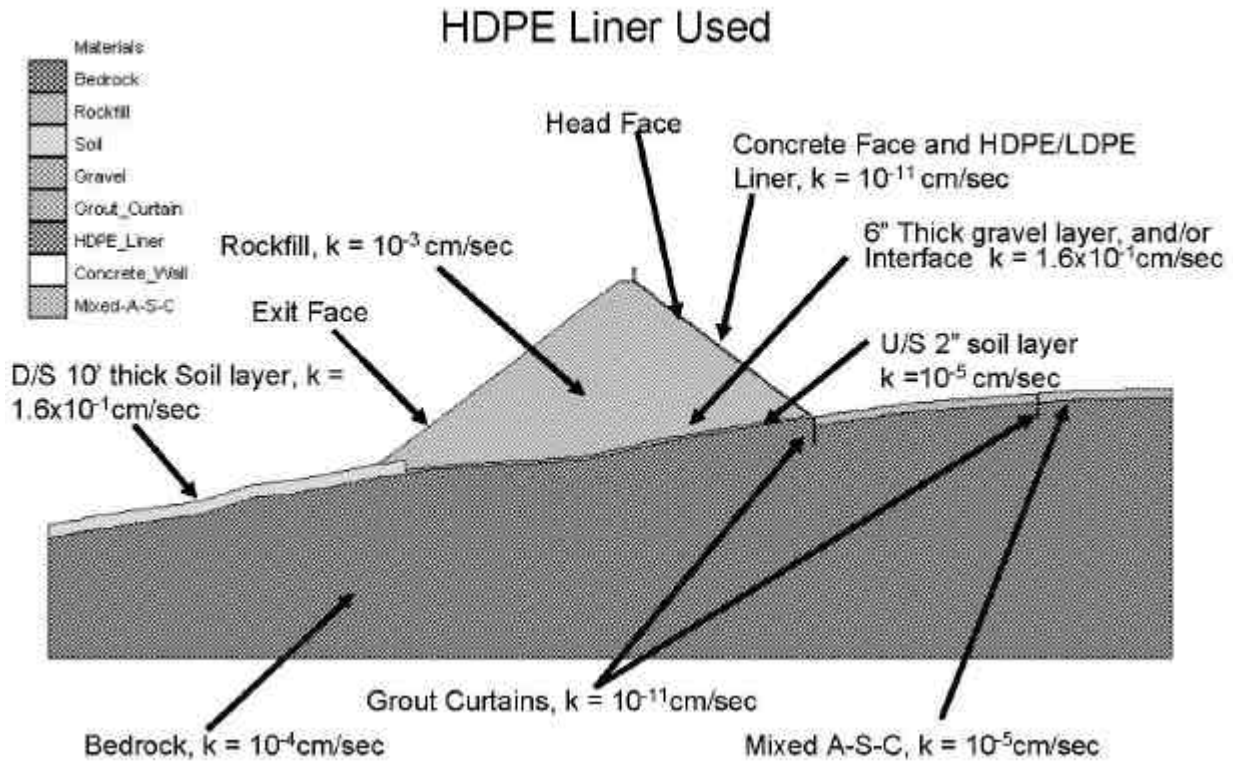


**FIGURE 8-17**

**BEST ESTIMATE SEEPAGE MODEL WITH LINER**

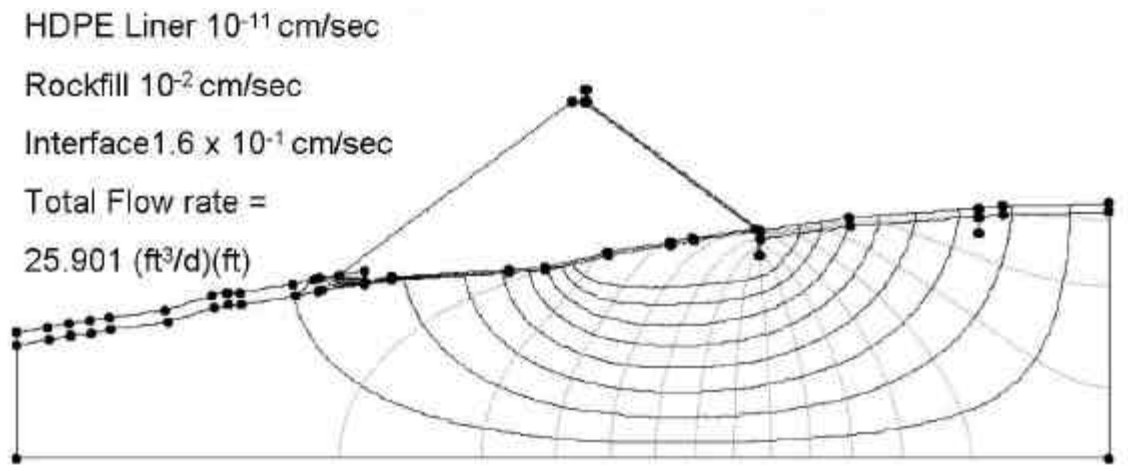


**FIGURE 8-18**

**FLOW NET FOR BEST ESTIMATE SEEPAGE MODEL WITH LINER**

The range of properties used in the parametric analysis of the seepage is summarized in *Table 8-1*. It is noted that we ran variations of the Best Estimate Model for those parameters determined to be significant with respect to overall seepage and overall flow net configuration.

**TABLE 8-1**  
**RANGE OF SEEPAGE ANALYSIS PARAMETRIC RUNS**

CASE NO.	ROCKFILL k (cm/sec)	SOIL k (cm/sec)	FILTER k (cm/sec)	OBSERVATIONS
1- BEST ESTIMATE	1 X 10 <sup>-3</sup>	1.6X10 <sup>-1</sup>	1.6X10 <sup>-1</sup>	NO PORE PRESSURE AT INTERFACE
2	1 X 10 <sup>-2</sup>	1.6X10 <sup>-1</sup>	1.6X10 <sup>-1</sup>	No pore pressure at interface
3	1 X 10 <sup>-4</sup>	1.6X10 <sup>-1</sup>	1.6X10 <sup>-1</sup>	No pore pressure at interface
4	1 X 10 <sup>-3</sup>	1.6X10 <sup>-2</sup>	1.6X10 <sup>-2</sup>	No pore pressure at interface
5	1 X 10 <sup>-3</sup>	1.6X10 <sup>-4</sup>	1.6X10 <sup>-4</sup>	Pore pressure at interface
6	1 X 10 <sup>-3</sup>	1.0X10 <sup>-5</sup>	1.6X10 <sup>-5</sup>	Pore pressure at interface

Note: 1. See *Appendix F* for related Calculations.

Not all parameters comprising the model are shown on the table as several were assessed interactively on the computer screen as not being significant. For example, we varied the permeability of the Two Grout Curtains and the Asphalt Pavement, but no significant change in the results was observed. Although our modeling shows that the assumed permeabilities of both the Grout Curtain and the Asphalt Pavement have a negligible effect on the phreatic surface, slight changes in pore pressures at the Dike/foundation interface can be expected, depending on the effectiveness of the Grout Curtains and the Asphalt Pavement..

Additionally, RIZZO observed that the initial grout curtain installed during the original construction had to be reinforced along its original alignment and then supplemented with an additional curtain further upstream. RIZZO also observed that the initial curtain, as well as the supplemental curtain, may have been inadequately designed, particularly with respect to depth. Similarly, RIZZO observed that the asphalt pavement in the vicinity of the Breach Area had to be repaired at least once after the original construction.

The results of these parametric runs presented in *Table 8-1* indicate that the permeability of the soil at the Dike/foundation interface and the Filters has a significant effect on the pore flow net and the pore pressure on the interface. To illustrate this point, we show below on *Figure 8-19* the flow net for Case 6 where the permeability of these two zones is postulated to be in the range of  $1 \times 10^{-4}$  cm/sec. The results also indicate that with the HDPE Liner in place, the permeability of the rock fill comprising the Dike is less important for the range of parameters that we considered.

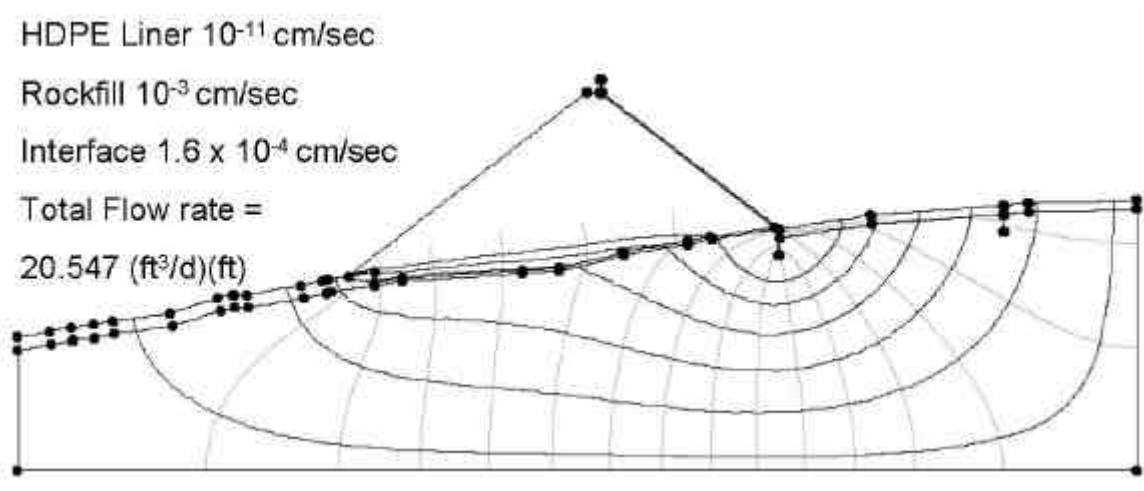


**FIGURE 8-19**

**FLOW NET FOR PARAMETRIC CASE 5**

**( $K_{\text{INTERFACE}} < K_{\text{ROCKFILL}}$ )**

**8.4 FORENSIC STABILITY ANALYSIS**

We have assessed the stability of the Rockfill Dike focusing on the geometry of the Breach Area and considering three Conditions:

**Condition A** Best Estimate Seepage conditions with Best Estimate soil and rock properties prior to installation of the geosynthetic liner as described in *Section 8.3.1* where our calibration efforts are described. Stability Analyses worksheets are provided in *Appendix F* for all Conditions.

**Condition B** Best Estimate Seepage with Best Estimate soil and rock properties plus a large number of parametric runs to gage sensitivity (after the installation of the geosynthetic liner). Seepage runs are described in *Section 8.3.2*.

This **Condition B** is indicative of conditions just prior to the December 14, 2005 Event.

**Condition C** Best Estimate Seepage with Best Estimate soil and rock properties plus a number of parametric runs to gage sensitivity (after the installation of the geosynthetic liner) and during the overtopping event of December 14, 2006.

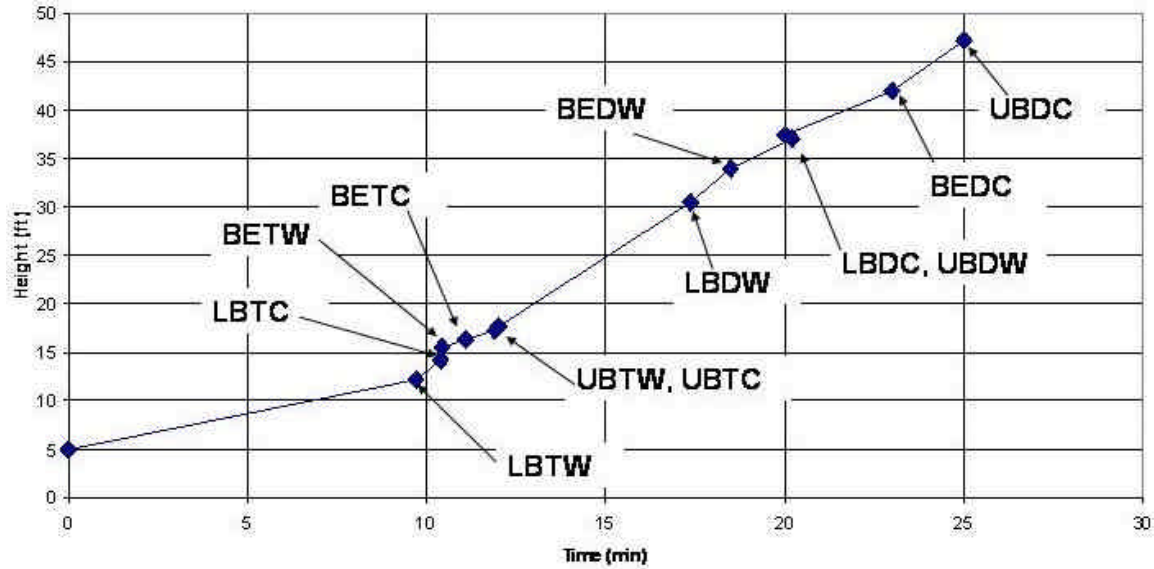
The computer program GSTABL7 was used to perform all Stability analysis (Gregory, 2003).

#### 8.4.1 Phreatic Surface & Pore Pressure Conditions for Stability Analysis

For **Condition A** as defined above, we used the phreatic surface shown on *Figure 8-16* whereby most of the Dike is saturated.

For **Condition B** as defined above, we used a variety of phreatic surfaces in a parametric manner to capture the range of possible seepage postulated conditions as listed on *Table 8-1*.

For **Condition C**, we interactively varied the phreatic surface with a series of runs starting with the **Condition B** case until the routine located a phreatic surface where the factor of safety against failure approached unity. As a check on the validity of the postulated failure surface from a timing perspective, we developed an infiltration model for the overtopping flow rates estimated for the Breach Area. This model with the results shown below on *Figure 8-20* shows our estimate of how the phreatic surface rose versus time during overtopping on December 14, 2005, and the estimated time when instability occurred - initially at the downstream toe and progressing up the downstream slope.



**LEGEND**

LB = Lower Bound	DW = Deep Wedge	DC = Deep Circular
BE = Best Estimate	TW = Toe Wedge	TC = Toe Circular

*Note: The saturation height is measured above the toe.*

**FIGURE 8-20**

**HEIGHT OF SATURATION ABOVE BEDROCK VERSUS TIME**

**8.4.2 Soil and Rock Properties**

*Figure 8-21* below indicates the properties selected for the Best Estimate Cases and the parametric runs and *Table 8-2* describes the basis for selection

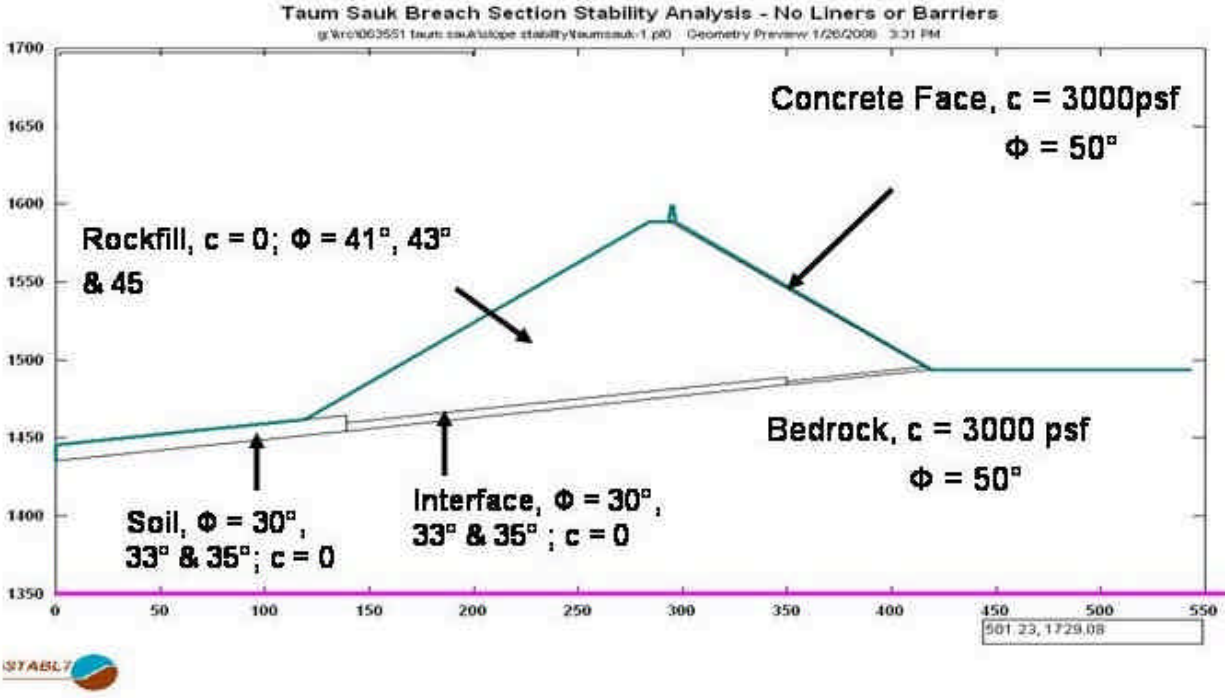


**FIGURE 8-21**

**SLOPE STABILITY ANALYSIS – MATERIAL PROPERTIES**

**TABLE 8-2****SUMMARY OF SOIL AND ROCK PROPERTIES**

<b>MATERIAL</b>	<b>LOWER BOUND</b>	<b>BEST ESTIMATE</b>	<b>UPPER BOUND</b>	<b>BASIS</b>
Foundation Soil at toe	c = 0 $\phi = 30^\circ$	c = 0 $\phi = 33^\circ$	c = 0 $\phi = 35^\circ$	Field Observations, Lab Tests & Calibration with Condition A
Filter Material	c = 0 $\phi = 30^\circ$	c = 0 $\phi = 33^\circ$	c = 0 $\phi = 35^\circ$	Field Observations & Calibration with Condition A
Bedrock	c = 3000 psf $\phi = 50^\circ$	c = 3000 psf $\phi = 50^\circ$	c = 3000 psf $\phi = 50^\circ$	Judgment No parametrics
Concrete Face	c = 3000 psf $\phi = 50^\circ$	c = 3000 psf $\phi = 50^\circ$	c = 3000 psf $\phi = 50^\circ$	Judgment No parametrics
Rockfill	c = 0 psf $\phi = 41^\circ$	c = 0 $\phi = 43^\circ$	c = 0 $\phi = 45^\circ$	LB – suggested by BOC BE – Back calculated from surface slides UB – Back calculated from Breach Area

**8.4.3 Results of Stability Analysis**

A summary of the stability analysis for the three above Conditions is provided below in three corresponding Tables. Details of each of the computer runs for the Best Estimate Properties are shown on *Figures 8-22 to 8-33*. Details for all of the computer runs are available in *Appendix F*.

**TABLE 8-3**

**SUMMARY OF STABILITY ANALYSIS  
FACTORS OF SAFETY  
CONDITION A**

<b>PHREATIC SURFACE</b>	<b>LOWER BOUND PROPERTIES</b>	<b>BEST ESTIMATE PROPERTIES</b>	<b>UPPER BOUND PROPERTIES</b>	<b>FAILURE TYPE</b>
Condition A	0.92	1.01	1.09	Deep Wedge - Fig. 8-22
Condition A	0.98	1.05	1.12	Deep Circle – Fig. 8-23
Condition A	1.06	1.15	1.13	Toe Wedge – Fig. 8-24
Condition A	1.11	1.13	1.21	Toe Circle – Fig. 8-25

It is noted that significant pore pressure probably existed at the Dike/foundation interface before the HDPE liner was installed. The results presented in *Table 8-3* indicate that the Rockfill Dike

prior to installation of the geosynthetic liner in the Breach Area was marginally stable where the material properties were in the range of selected Lower Bounds.

We note that the elevated phreatic surface analyzed in Condition A represents estimated seepage conditions for the Rockfill Dike prior to installation of the synthetic liner. The assumed phreatic surface was estimated based on available information and data pertaining to the permeability of the various zones and was back-calculated to match the pre-liner recorded seepage quantities. Although an increase in pore pressure resulting from leaks through cracks in the concrete face would serve to diminish the factor of safety against stability failure of the Rockfill Dike (as shown in **Table 8-3**), the placement of the synthetic liner in the fall of 2004 diminished, and probably eliminated, the leaks through the concrete face. Thus, any pore pressure attributed to leakage through the concrete face prior to the installation of the synthetic liner would likely have been dissipating at the time of the Event in December 2005. It is our opinion that the actual phreatic surface just prior to the Event was somewhere between that shown on **Figure 8-16** (pre-liner) and **Figure 8-18** (post-liner).

If any residual pore pressures remained, then leaks through cracks or expansion joints in the concrete on the upstream face of the Rockfill Dike may have been a secondary contributing cause of the Event from the perspective that leaks through cracks or expansion joints could have caused increased pore pressures at the Dike/foundation interface. However, we are unable to determine if these pore pressures had fully drained prior to the event.

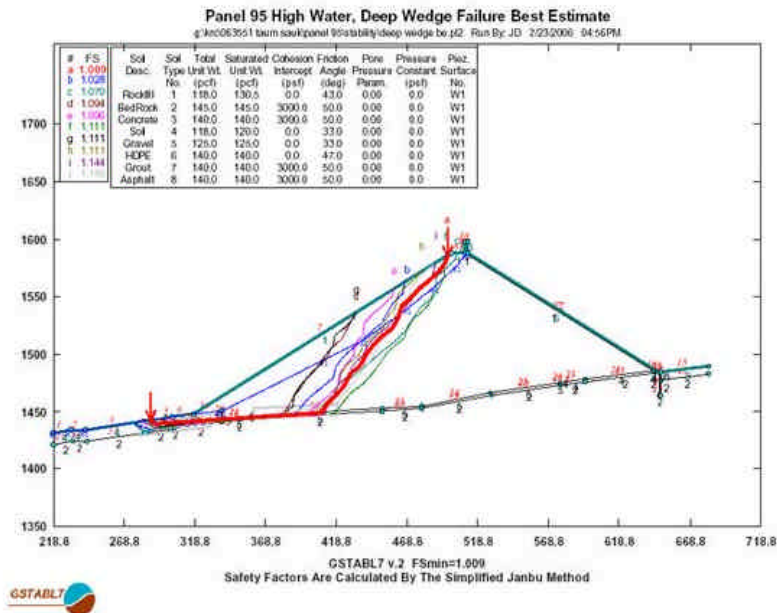


**FIGURE 8-22**

**DEEP WEDGE FAILURE – CONDITION A  
(BEST ESTIMATE PROPERTIES)**

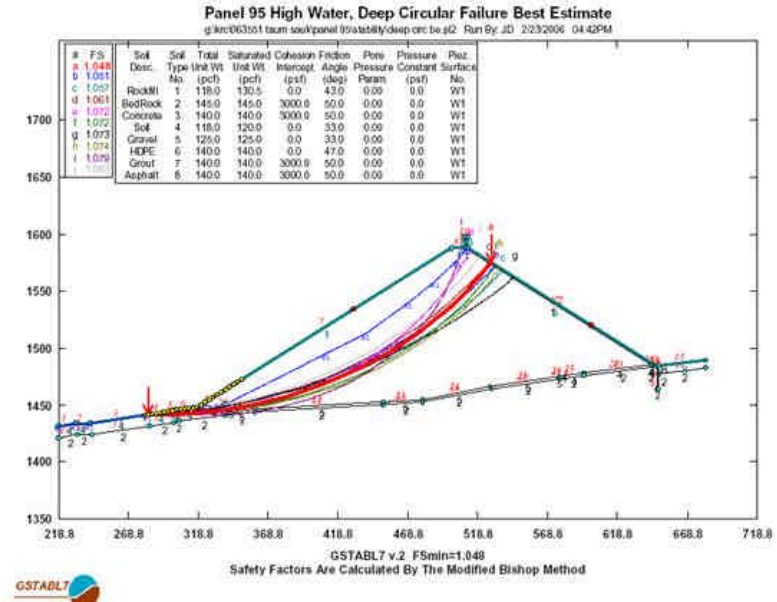


**FIGURE 8-23**

**DEEP CIRCLE FAILURE – CONDITION A  
(BEST ESTIMATE PROPERTIES)**

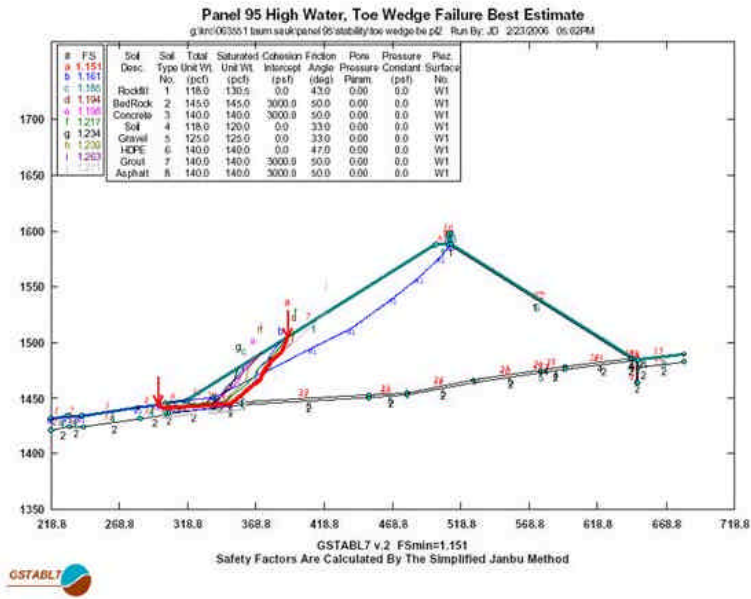


**FIGURE 8-24**

**TOE WEDGE FAILURE – CONDITION A  
(BEST ESTIMATE PROPERTIES)**

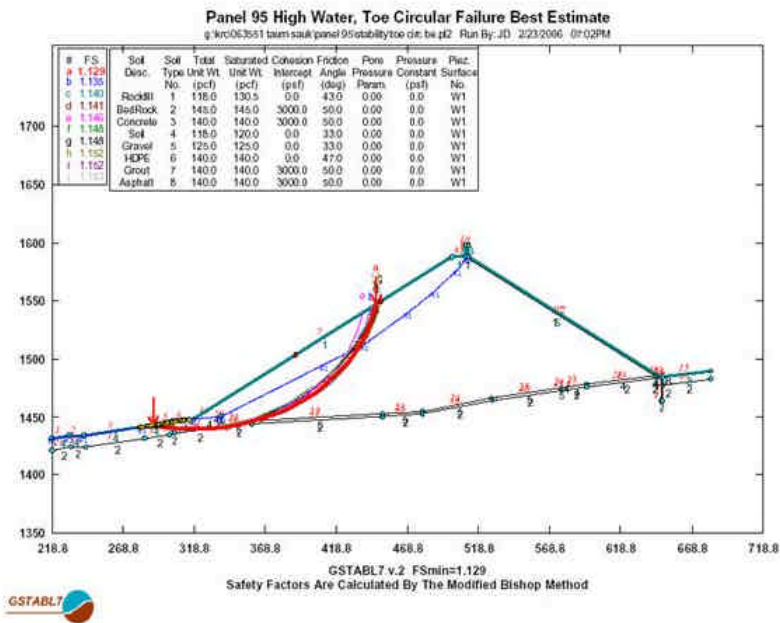


**FIGURE 8-25**

**TOE CIRCLE FAILURE – CONDITION A  
(BEST ESTIMATE PROPERTIES)**

**TABLE 8-4**

**SUMMARY OF STABILITY ANALYSIS  
FACTORS OF SAFETY  
CONDITION B**

PHREATIC SURFACE	LOWER BOUND PROPERTIES	BEST ESTIMATE PROPERTIES	UPPER BOUND PROPERTIES	FAILURE TYPE
Condition B	1.24	1.35	1.45	Deep Wedge – Fig. 8-26
Condition B	1.23	1.33	1.42	Deep Circle – Fig. 8-27
Condition B	1.10	1.21	1.30	Toe Wedge – Fig. 8-28
Condition B	1.11	1.23	1.32	Toe Circle – Fig. 8-29

The results presented in *Table 8-4* indicate that the Rockfill Dike after installation of the geosynthetic liner in the Breach Area resulted in a slightly higher factor of safety. However, the results indicated that the section would still not meet FERC criteria for stability under static conditions for maximum storage pool (i.e., FS=1.5) (FERC, 1991). Although dynamic analyses have not been run, past experience suggests a high probability of failure under significant earthquake loading. The addition of a pseudo-static earthquake coefficient would result in a lower factor of safety approaching one. A pseudo static factor less than about 1.3 results in some amount of permanent deformation which increases exponentially with successively lower factors of safety.

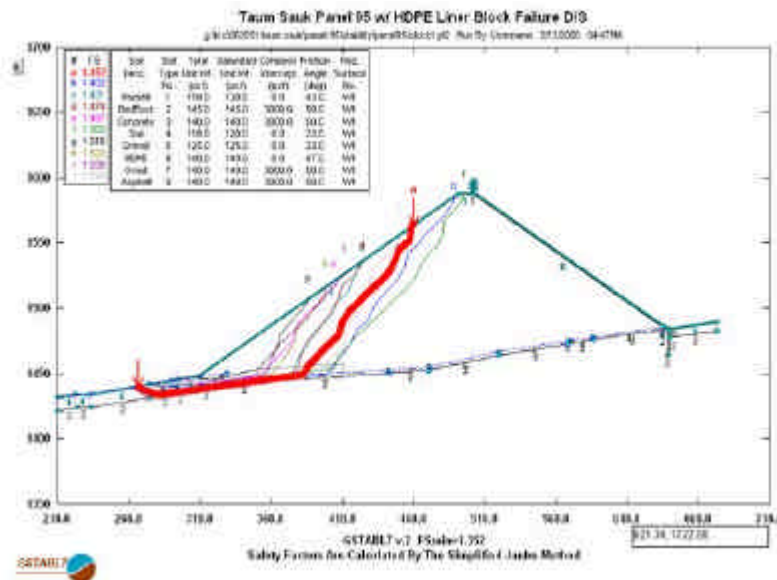


**FIGURE 8-26**

**DEEP WEDGE FAILURE – CONDITION B  
(BEST ESTIMATE PROPERTIES)**

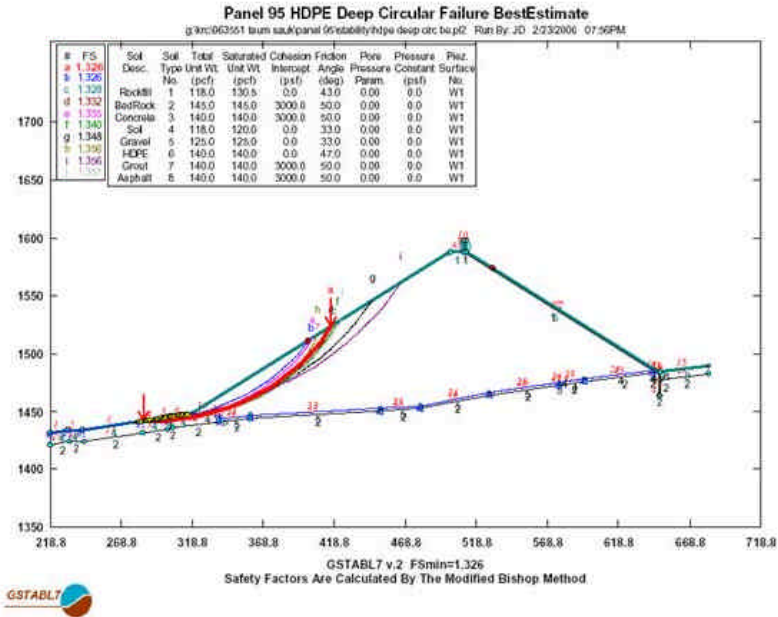


**FIGURE 8-27**

**DEEP CIRCLE FAILURE – CONDITION B  
(BEST ESTIMATE PROPERTIES)**

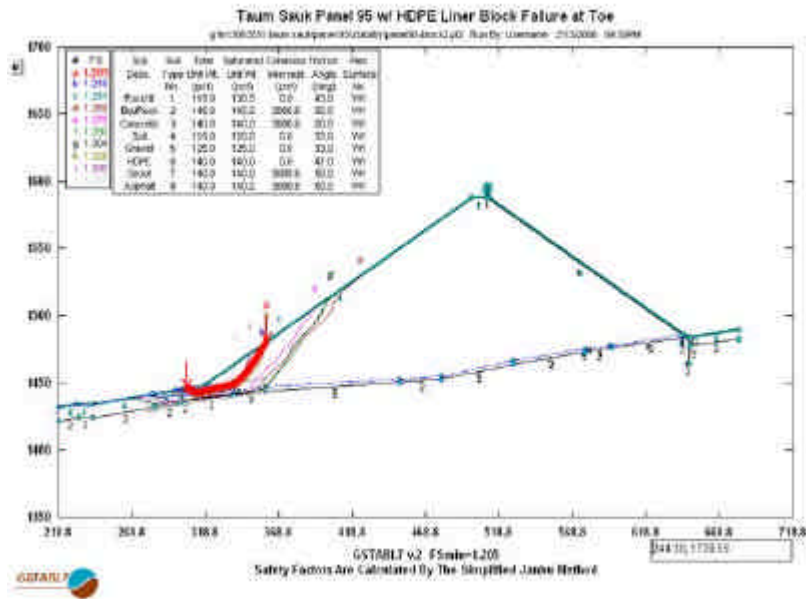


**FIGURE 8-28**

**TOE WEDGE FAILURE – CONDITION B  
(BEST ESTIMATE PROPERTIES)**

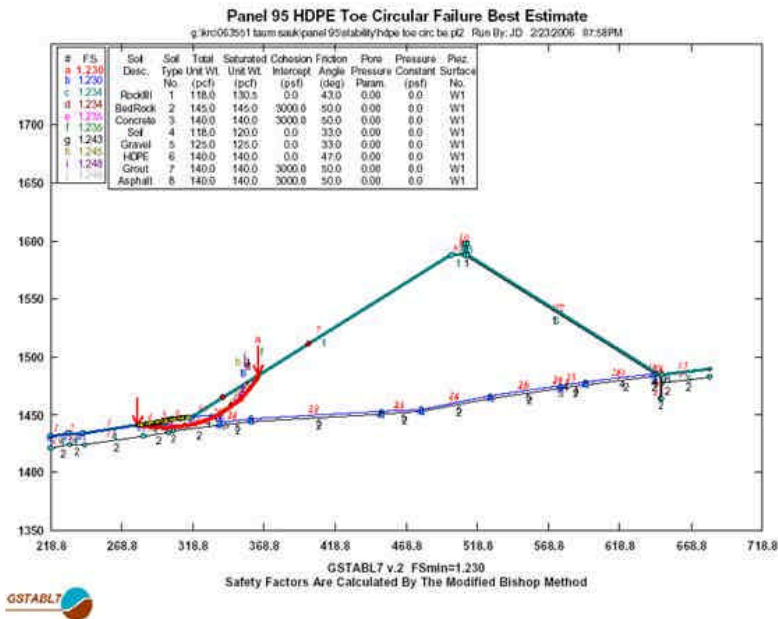


**FIGURE 8-29**

**TOE CIRCLE FAILURE – CONDITION B  
 (BEST ESTIMATE PROPERTIES)**

**TABLE 8-5**

**SUMMARY OF STABILITY ANALYSIS  
 HEIGHT OF PHREATIC SURFACE ABOVE BEDROCK  
 TO PRODUCE FACTOR OF SAFETY OF 1.0  
 CONDITION C**

<b>ESTIMATED TIME OF FAILURE (BE PROPERTIES)</b>	<b>LOWER BOUND PROPERTIES</b>	<b>BEST ESTIMATE PROPERTIES</b>	<b>UPPER BOUND PROPERTIES</b>	<b>FAILURE TYPE</b>
18 min	31 ft	34 ft	37 ft	Intermediate to Deep Wedge - Fig. 8-30
23 min	37 ft	42 ft	47 ft	Deep Circle (Infinite Slope) – Fig. 8-31
11 min	12 ft	16 ft	17 ft	Toe Wedge – Fig. 8-32
12 min	14 ft	16 ft	17 ft	Toe Circle – Fig. 8-33

Notes:

1. The height of the phreatic surface is measured above the bedrock directly at the downstream toe.
2. The Estimated Time of Failure is our estimate when the Failure Type occurred. See *Figure 8-20*.

The first line of Table 8-5 indicates that RIZZO estimates that it would take about 18 minutes for the phreatic surface to increase to 34 feet above the bedrock. With the phreatic surface at this level, an intermediate to deep wedge type failure would have a factor of safety of one. Based on the analyses presented, it is RIZZO's opinion that the failure began at the toe (with either a wedge or circular failure). **Table 8-5** indicates that the toe failure condition reached a factor of safety of one when the phreatic surface was in the range of 12 feet to 17 feet above the bedrock. This occurred in the range of 10 to 13 minutes after the Upper Reservoir level reached El. 1597. The results also indicate that while failure began at the toe, probably exacerbated by run off down the slope, it rapidly progressed up slope within minutes.

The increase in phreatic surface within the Dike on the day of the Event is directly attributed to the overtopping flow. RIZZO is unable to measure or calculate with precision the level and shape of the phreatic surface just prior to the overtopping. The analyses summarized in **Table 8-5** assumed that the initial (pre-overtopping) phreatic surface was about five feet above bedrock. In terms of the Barriers presented in **Section 5.0**, this assumed initial phreatic surface might have been elevated by an ineffective Grout Curtain, Asphalt Pavement, or the Foundation Filters. Performance of the Foundation Filters was discussed and dismissed in **Section 8.3.1** as non-causal. If, on the other hand, the Grout Curtains and/or Asphaltic Pavement were ineffective and causing leakage through or seepage under, either could have impacted the level or the shape of the pore pressure distribution at the Dike/foundation interface. An increase in pore pressure would have diminished the (pre-overtopping) factor of safety against stability failure of the Rockfill Dike and possibly result in a faster time to failure as compared to the times presented in **Table 8-5**. However, it is RIZZO's opinion that neither the Grout Curtains nor the Asphalt Pavement played a substantial role in the Event and that, at best, an ineffective Grout Curtain or an ineffective Asphalt Pavement may have been a secondary contributing cause.

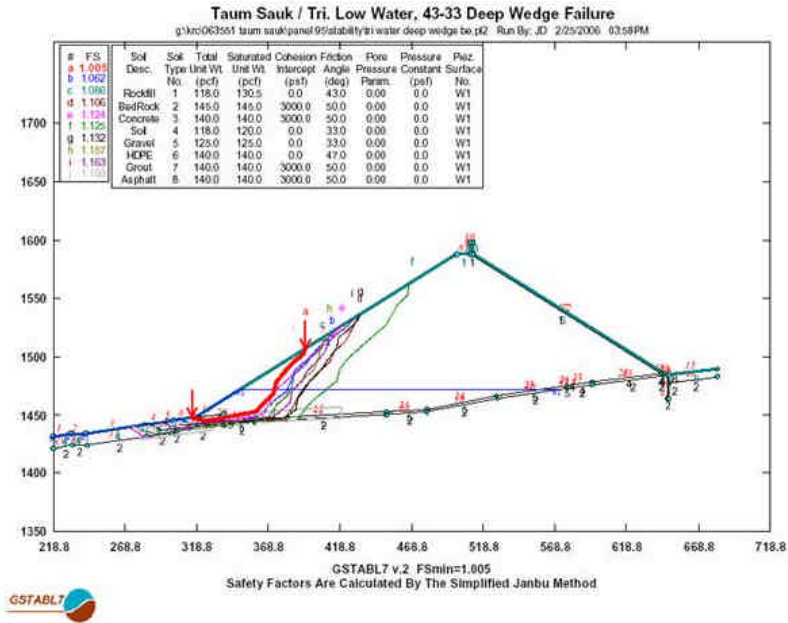


**FIGURE 8-30**

**INTERMEDIATE TO DEEP WEDGE FAILURE – CONDITON C  
 (BEST ESTIMATE PROPERTIES)**

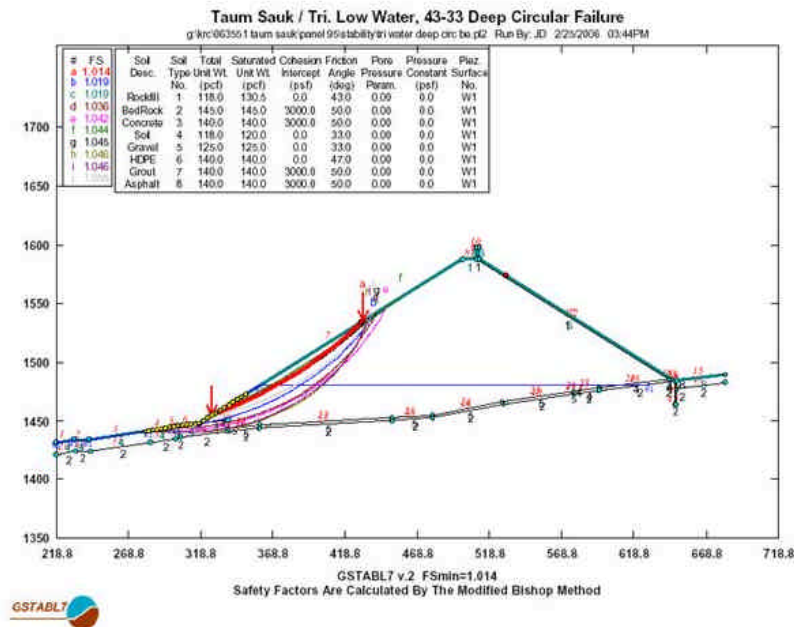


**FIGURE 8-31**

**DEEP CIRCLE (INFINITE SLOPE) FAILURE – CONDITION C  
 (BEST ESTIMATE PROPERTIES)**

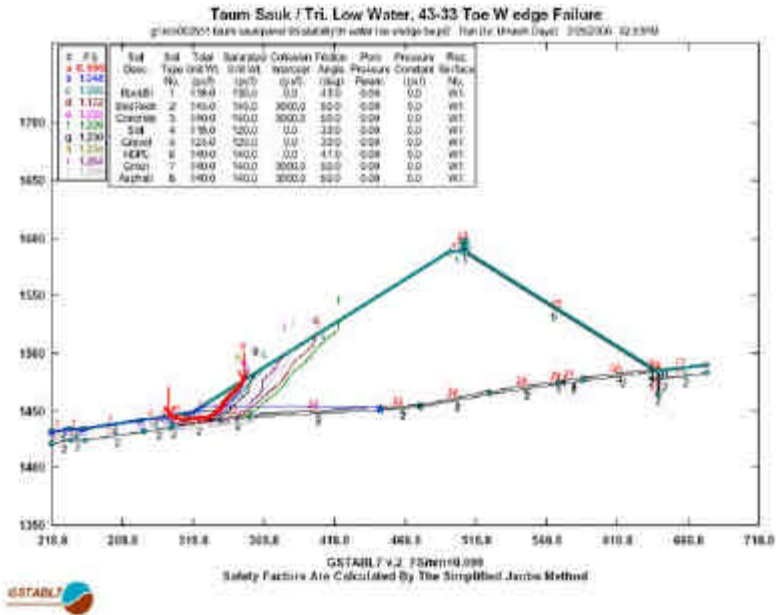


**FIGURE 8-32**

**TOE WEDGE FAILURE – CONDITION C  
 (BEST ESTIMATE PROPERTIES)**

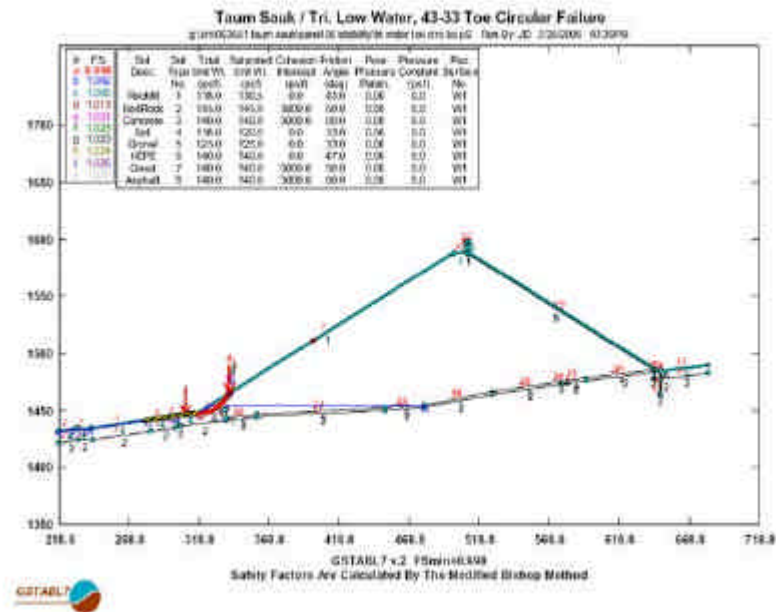


**FIGURE 8-33**

**TOE CIRCLE FAILURE – CONDITION C  
 (BEST ESTIMATE PROPERTIES)**

## 8.5 PREVIOUS SLOPE STABILITY ANALYSIS

Slope stability of the Upper Reservoir Dike was previously evaluated (by others) as part of the normal dam safety and inspection process. These analyses were included in the latest Part 12 Report (MWH, 2003) and the results showed that the Dike apparently met current dam safety requirements as per the FERC guidelines. In this section, we compare and contrast the existing analysis as compared to the post-incident analysis summarized in *Section 8.4*.

Based on our review of these analyses, RIZZO has the following comments:

**Phreatic Surface:** In the previous analysis, it was assumed that no pore pressure exists in the rockfill (assumed a dry slope condition). While this is often consistent with a concrete faced rockfill dam, it is not appropriate for the Dike at Taum Sauk. The high percentage of fines within a rockfill has the effect of increasing pore pressures within a dam or dike. Substantial seepage was flowing through the Taum Sauk Dike with estimates of seepage ranging from 10 to 40 cfs with an average of about 20 cfs. When this seepage flow encountered fines, increased pore pressure resulted.

Utilizing the finite element-based SEEP2D modeling program and measured seepage quantities, RIZZO developed phreatic surfaces consistent with the concrete-lined and the HDPE-lined upstream face. These phreatic surfaces were used to calculate slope stability factors of safety. It is noted that the phreatic surface has an impact on the factor of safety (as the phreatic surface increases, the FS decreases).

**Soil Properties:** In the previous analysis, one type of material is assumed for the entire Rockfill Dike having shear strength properties of friction angle ( $\phi$ ) equal to 45 degrees with no cohesion. However, the original design drawings show three distinct soil layers within the downstream slope of the embankment; namely, rockfill, a filter layer, and unexcavated soil. RIZZO has performed a parametric investigation of the slope stability analyses assuming lower bound, best estimate, and upper bound material properties for each of these layers. Those material properties are listed in *Table 8-2*. The estimated material property values were back-calculated from the failed slopes and confirmed with laboratory test results. The soil and filter layers located atop the weathered rock have much lower strength values in comparison to rockfill material. This foundation layer critically governs the factor of safety for slope stability. Lower shear strength values for the foundation material yields lower factors of safety.

**Wedge versus Circular Failures:** The original analyses assumed uniform strength properties for the embankment and the foundation. In this case, circular failure surfaces control. However, in the case analyzed herein, the foundation layer is significantly weaker than the overlying embankment. In this case, a wedge failure (with a resulting lower factor of safety) governs the slope stability analysis.

**Actual Site Conditions:** Inclusion of actual site conditions, as stated above, will result in a lower factor of safety as compared to the original analyses.

**Independent Check:** As a check, RIZZO has independently performed the slope stability analyses using the same geometry and strength properties as used in the original stability calculations—not the properties that RIZZO interprets to be appropriate. The results are presented on *Figure 8-34*. These results show a factor of safety of 1.5 as reported in the original calculations prepared by the original designer.

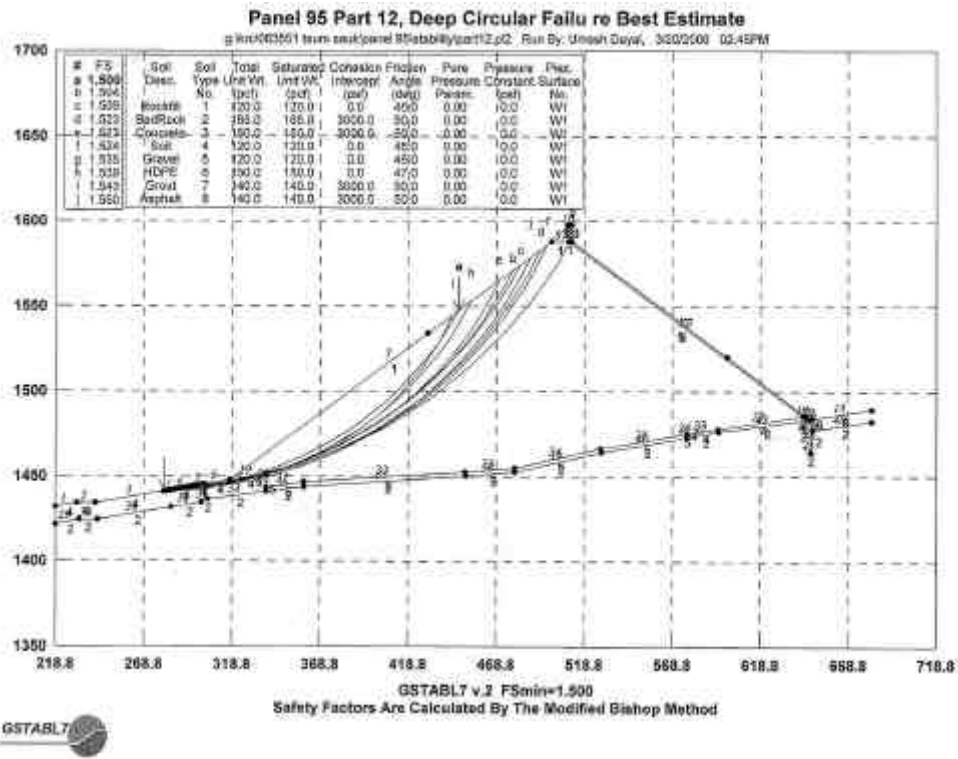


**FIGURE 8-34**

**CHECK – ORIGINAL STABILITY ANALYSIS  
 FACTOR OF SAFETY EQUAL 1.5**